

# Polymer-tethered membranes as quantitative models for the study of integrin-mediated cell adhesion†

Oliver Purruicker,<sup>a</sup> Stefanie Gönnerwein,<sup>a</sup> Anton Förtig,<sup>b</sup> Rainer Jordan,<sup>\*bc</sup> Monika Rusp,<sup>a</sup> Michael Bärmann,<sup>a</sup> Luis Moroder,<sup>d</sup> Erich Sackmann<sup>a</sup> and Motomu Tanaka<sup>\*ae</sup>

Received 22nd August 2006, Accepted 27th October 2006

First published as an Advance Article on the web 23rd November 2006

DOI: 10.1039/b612069e

Here we report a remarkable enhancement in the adhesion strength of transmembrane cell receptors, human platelet integrin, in a new class of supported lipid membranes, which are separated from the solid substrates by linear polymer spacers. The amphiphilic polymer tether consists of linear hydrophilic poly(2-oxazoline) chains of defined length (degree of polymerization  $n = 104$ ,  $M_w/M_n = 1.30$ ), whose chain termini are functionalized with the tri-functional silane surface coupling group and hydrophobic  $n$ -alkyl chains as membrane anchors (lipopolymers). As a model of test cells, giant lipid vesicles were functionalized with synthetic ligand molecules containing the RGD sequence, and the free energy of adhesion  $\Delta g_{\text{ad}}$  between the integrin-doped tethered membrane and the vesicle was measured using a micro-interferometry technique. It has been demonstrated that the adhesion function of integrin receptors in these polymer-tethered membranes is 30 times stronger than those incorporated into membranes directly deposited onto solid substrates (solid-supported membranes). The obtained results demonstrate that linear lipopolymer spacers provide a fluid and non-denaturing environment for the incorporated cell receptors and allow quantitative modelling of cell adhesion processes.

## Introduction

Planar lipid membranes deposited on solid substrates (supported membranes) can serve as plasma membrane models to study the functions of membrane proteins.<sup>1–5</sup> However, despite remarkable progress, the direct deposition of supported membranes onto solid substrates (solid-supported membranes) often causes undesired denaturing of transmembrane proteins, whose functional headgroups protrude up to tens of nm from the membrane surfaces. This problem can be avoided by separating the membrane from the solid substrate using soft polymeric materials that rest on the substrate and support the membrane. This approach significantly reduces the frictional coupling between membrane-incorporated proteins and the solid support, and hence the risk of protein denaturation.<sup>4,6,7</sup>

More recently, we reported a new class of supported lipid bilayer membranes that are separated from the substrate by flexible poly(2-methyl-2-oxazoline) lipopolymer “tethers”.<sup>8,9</sup> In contrast to solid-supported membranes, the tethers of defined length (degree of polymerization  $n = 14–104$ ;

polydispersity indices  $\text{PDI} = 1.05–1.30^{10}$ ) facilitate a systematic improvement in the homogeneity of the distribution and the lateral diffusivity of incorporated transmembrane proteins,<sup>11</sup> which can be interpreted as the reduction of frictional coupling between the proteins and the underlying solid substrate.

Integrin  $\alpha_{\text{IIb}}\beta_3$  receptors are transmembrane, cell adhesion molecules expressed on human blood platelets, which play a critical role in thrombosis and haemostasis.<sup>12</sup> The integrin  $\alpha_{\text{IIb}}\beta_3$  molecule (molecular mass of about 240 kDa) has a small intracellular domain and a large extracellular domain ( $8 \times 12 \text{ nm}^2$ ), which bears a specific binding site for Arg-Gly-Asp (RGD) sequences of fibrinogen, fibronectin, von Willebrand's factor and vitronectin. In our previous account,<sup>13</sup> we demonstrated the presence of 5–10 nm thick films of regenerated cellulose leads to a significant improvement in lateral homogeneity and diffusivity of the transmembrane cell receptors. The quantitative measurement of the free energy of adhesion,  $\Delta g_{\text{ad}}$ , per unit area indicated a remarkable enhancement in the adhesion function of integrin on polymer supports.

## Results and discussion

In this study, we utilized the polymer-tethered membranes as the quantitative model system to measure the free energy of adhesion,  $\Delta g_{\text{ad}}$ , between the receptor-functionalized membrane and a giant lipid vesicle with specific ligands (Fig. 1). The ligand molecule used here was a lipid coupled to a cyclic hexapeptide containing the RGD sequence that is specifically recognized by integrin  $\alpha_{\text{IIb}}\beta_3$ .<sup>14</sup>

Adopting the classical Young–Dupré equation,<sup>15–17</sup>

$$\Delta g_{\text{ad}} = \gamma(1 - \cos \alpha) \quad (1)$$

<sup>a</sup>Lehrstuhl für Biophysik E22, Technische Universität München, 85748, Garching, Germany

<sup>b</sup>Lehrstuhl für Makromolekulare Stoffe, Department Chemie, Technische Universität München, 85748, Garching, Germany. E-mail: rainer.jordan@ch.tum.de

<sup>c</sup>Department of Chemistry, Chemical Engineering and Materials Science, Polytechnic University, Brooklyn, NY, 11201, USA

<sup>d</sup>Max-Planck-Institut für Biochemie, 82152, Martinsried, Germany

<sup>e</sup>Lehrstuhl für Biophysikalische Chemie, Physikalisch-Chemisches Institut, Ruprecht-Karls-Universität Heidelberg, 69120, Heidelberg, Germany

† This paper is part of a *Soft Matter* themed issue on Proteins and Cells at Functional Interfaces. Guest editor: Joachim Spatz.

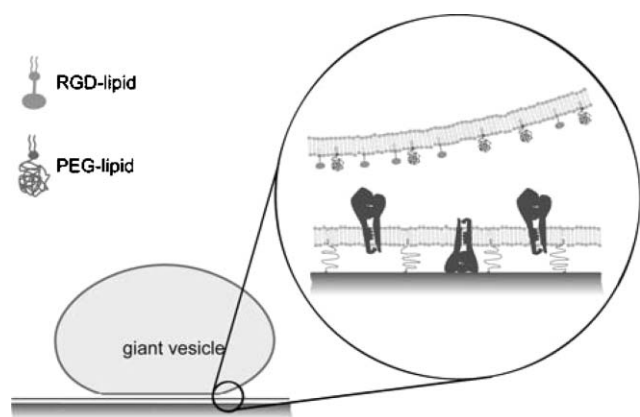


**Fig. 1** A giant lipid vesicle adhering to a polymer-tethered membrane with incorporated integrin  $\alpha_{11b}\beta_3$ . The specific binding is generated by ligands bearing the RGD sequence, whereas the PEG lipids prevent non-specific adhesion.

the free energy of adhesion can be determined from the equilibrium vesicle contour close to the substrate using the micro-interferometry technique,<sup>18–20</sup> where  $\alpha$  is the contact angle defined in Fig. 2(c), and  $\gamma$  is the lateral membrane tension. Here, the tension of the fluid vesicle membrane is assumed to be constant.

Fig. 2(a) illustrates a reflection interference contrast microscopy (RICM) image of an adherent vesicle on a polymer-tethered membrane. The white line coincides with the contact line, where the interferogram was analyzed (Fig. 2(b)). From the intensity profile, the height profile of the vesicle can be calculated (Fig. 2(c)).

As one can see in Fig. 2(c), the quantitative determination of the effective contact angle  $\alpha$  is often found to be difficult experimentally. To overcome this problem, another length scale  $\lambda$  was introduced to analyze the height profile of the vesicle in the vicinity of the contact line, according to the theory of Bruinsma:<sup>21</sup>

$$h(x) = \alpha(x - \lambda) + \alpha\lambda \exp(-x/\lambda), \quad (2)$$

where  $x$  is defined as the distance from the vesicle–surface contact (Fig. 2(c)),  $\alpha$  is the macroscopic contact angle between the membrane and the substrate, and  $\lambda$  is the capillary length,

$$\lambda = (\gamma/\kappa)^{0.5}. \quad (3)$$

$\lambda$  is a measure of the length over which the height profile of the membrane is dominated by the bending elasticity of the membrane. In other words, the vesicle shape is dominated only by tension when  $x > \lambda$ . The geometric parameters  $\alpha$  and  $\lambda$  can be determined from the RICM image for each location along the rim of the adhesion disc.<sup>20</sup> The capillary length  $\lambda$  is determined by the distance between  $x = 0$  and the intersection of the extrapolation of the fit to the membrane contour at  $x \gg \lambda$  and the  $x$ -axis. The zero point ( $x = 0$ ) is defined as the onset of the deflection of the membrane (Fig. 2(c)). The bending stiffness  $\kappa$  is assumed to be  $100 k_B T$  for vesicles containing 50 mol% DMPC and 50 mol% cholesterol.<sup>22</sup> According to the

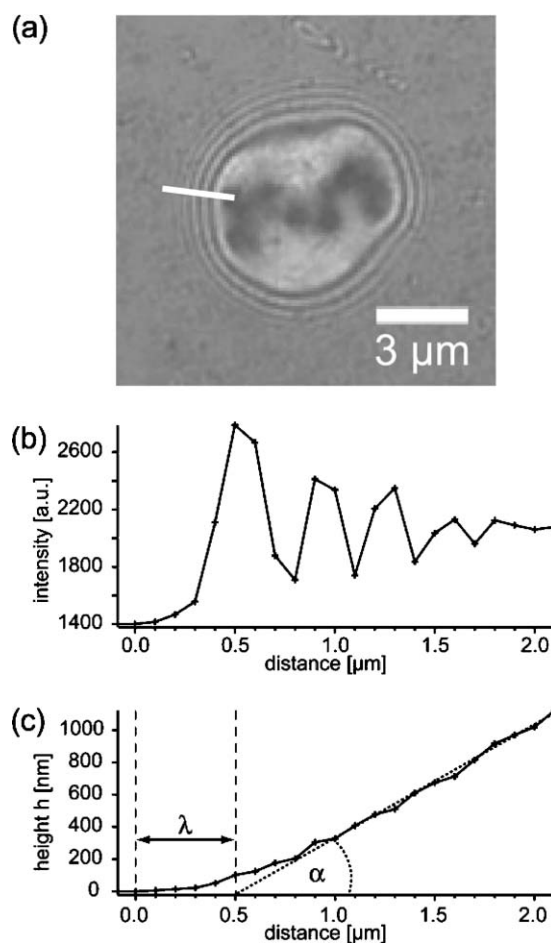


**Fig. 2** (a) The reflection interference contrast microscopy (RICM) interferogram (averaged over 20 images taken during a period of  $\approx 2$  s) of a giant vesicle containing 1 mol% RGD lipid and 1 mol% PEG lipid, adhering to a membrane with 0.5 mol% DS-PMO<sub>x104</sub>-Si in the underlayer and incorporated integrin  $\alpha_{11b}\beta_3$ . The dark areas indicate strongly adherent membrane patches. Interference fringes around the contact area show lines of equal height of the vesicle membrane above the substrate. (b) The intensity profile along the contact line, indicated in the interferogram in Fig. 1(a). (c) The local height profile can be reconstructed from the intensity profile, which enables the definition of the contact angle  $\alpha$  and the characteristic capillary length  $\lambda$ . The zero point of the  $x$ -axis ( $x = 0$ ) is determined by the onset of the upward deflection of the vesicle membrane from the substrate.

Young equation (eqn 1), the local free energy of adhesion  $\Delta g_{ad}$  can be determined at several positions of the rim.

In order to prevent non-specific adhesion of the vesicle onto the surface due to van der Waals attractions, the vesicle membrane was passivated with small amounts (1 or 2 mol%) of lipopolymers with poly(ethylene glycol) headgroups (PEG lipids), which create a “stealth” layer.<sup>17</sup> Here, the obtained adhesion free energy  $\Delta g_{ad}$  is smaller than the specific adhesion energy of the receptor–ligand pairs per unit area  $W_{ad}$ , since the repeller molecules are excluded from the region of tight adhesion, which creates an osmotic pressure difference  $\Delta\pi_R = k_B T \Delta c_R$  between the adherent and non-adherent parts of the vesicle membrane.<sup>16,17,23</sup>

$$\Delta g_{ad} = W_{ad} - \Delta\pi_R. \quad (4)$$

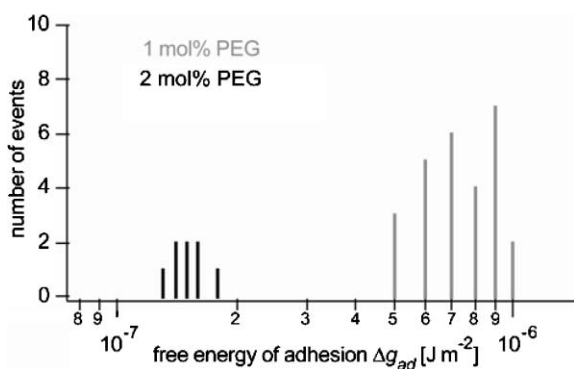


Fig. 3 A histogram of the measured free energies of adhesion of vesicles containing 1 and 2 mol% of repeller lipids (PEG lipids).

In Fig. 3, the histograms of measured values of  $\Delta g_{ad}$  of vesicles containing 1 and 2 mol% PEG lipids as steric “repellers” are presented. From the results extracted from more than eight individual positions of the rim, the mean values of  $\Delta g_{ad}$  can be calculated for each of the repeller concentrations. Owing to the linear dependence of  $\Delta g_{ad}$  on the repeller concentration  $\Delta c_R$  (eqn 4), the specific binding energy  $W_{ad}$  can be obtained by linear extrapolation of  $\Delta g_{ad}$  vs.  $\Delta c_R$  to  $\Delta c_R = 0$ , yielding the specific binding energy  $W_{ad} \approx 1.4 \times 10^{-6} J m^{-2}$ .

From the ratio of integrins to phospholipids in the lipid vesicles of 1 : 6200 (see Experimental section), the surface density of integrin can be estimated to be  $2.3 \times 10^{14} m^{-2}$ . Assuming that about 50% of the integrin receptors are facing their extracellular domain with the RGD recognition site towards the bulk electrolyte, the density of integrin potential binding sites is calculated to be  $1.2 \times 10^{14} m^{-2}$ †. Using the specific adhesion energy per unit area  $W_{ad} \approx 1.4 \times 10^{-6} J m^{-2}$ , one can estimate the specific interaction energy of an integrin–RGD pair to be  $U \approx 1.2 \times 10^{-20} J$ , corresponding to  $U \approx 3 k_B T$ . This value is about one third of the binding energy of integrin–RGD pairs obtained from the biochemical assay,  $U \approx 10 k_B T$ ,<sup>14</sup> and is approximately 30 times larger than the corresponding value measured on solid-supported membranes.<sup>13</sup> Thus, it has been concluded that the linear polymer spacers provide a lubricating layer between the substrate and the lipid bilayer membrane that reduces frictional coupling between the incorporated integrin receptors and the substrate surface‡. This significantly improves not only the homogeneity of the lateral distribution but also the adhesion function of the incorporated cell receptors. This demonstrates that such model biomembranes can be used as quantitative models of the cell surface,<sup>4</sup> which allows the expression of a defined number of functional molecules without losing their natural functions.

† This assumption is based on the random protein orientation as a result of membrane disruption by surfactants during the protein incorporation, observed by cryo-electron microscopy experiments.<sup>14</sup> In this paper, we also corrected the adhesion function of integrin calculated in ref. 13 for comparison.

‡ The substrate–membrane distance in the presence of the lipopolymer-tether ( $n = 104$ ) was recently measured in the absence and presence of integrin using fluorescence interference contrast microscopy to be about 5 nm (Purrucker *et al.*, unpublished results).

## Experimental

The synthesis and characterization of the poly(2-methyl-2-oxazoline) lipopolymers were reported previously.<sup>8,24</sup> They consist of a distearoyl lipid moiety, a trimethoxysilane surface anchoring group and a flexible, hydrophilic poly(2-methyl-2-oxazoline) polymer chain with a degree of polymerization of  $n = 104$  (DS-PMO<sub>x104</sub>-Si) and a polydispersity index PDI = 1.30 as measured by gel permeation chromatography. As matrix lipids, 1-stearoyl-2-oleoyl-*sn*-glycero-3-phosphocholine (SOPC), 1,2-dimyristoyl-*sn*-glycero-3-phosphocholine (DMPC), and 1,2-dimyristoyl-*sn*-glycero-3-[phospho-*rac*-(1-glycerol)] (DMPG), were used (Avanti Polar Lipids, Alabaster, USA). Freshly distilled and deionized water (Millipore, Molsheim, France,  $R > 18 M\Omega cm$ ) was used as the subphase of the Langmuir–Blodgett (LB) trough. Buffer solutions were prepared with tris(hydroxymethyl)amino-methane (Tris), purchased from Roth GmbH (Karlsruhe, Germany). All other chemicals were purchased from Sigma-Aldrich (Munich, Germany) and used without further purification. Glass cover slides (24 × 24 mm) from Karl Hecht KG (Sondheim, Germany) were used as solid supports. The polymer-tethered lipid membranes with reconstituted transmembrane cell receptors, integrin  $\alpha_{IIB}\beta_3$ , were prepared in two steps.<sup>8,24</sup> The proximal leaflet of the lipid membrane was deposited by Langmuir–Blodgett transfer of a lipid (99.5 mol% SOPC)/lipopolymer (0.5 mol% DS-PMO<sub>x104</sub>-Si) monolayer onto a cover slide. The distal leaflet was prepared by fusion of proteoliposomes containing integrin  $\alpha_{IIB}\beta_3$  and DMPC/DMPG matrix lipids (1 : 1 molar). The preparation of proteoliposomes was reported elsewhere.<sup>8,14,24</sup>

The ratio of integrins to phospholipids in proteoliposome suspensions was quantified by separate determination of the protein concentration by UV spectroscopy measurements, following the procedure reported by Bradford,<sup>25</sup> and the lipid concentration measured by phosphate analysis according to Fiske and Subbarow<sup>26</sup> and Bartlett.<sup>27</sup> The integrin concentration was found to be  $\approx 41$  nM, whereas the lipid concentration was  $\approx 250$   $\mu M$ , yielding a molar ratio of [integrin] : [lipids]  $\approx 1$  : 6200. Since proteoliposomes were spread onto LB monolayers of lipids and small fractions of lipopolymers, the amount of lipid per incorporated integrin roughly doubles. Therefore, the ratio of reconstituted proteins to lipids per surface area is  $X_i \approx 1$  : 6200. Assuming an average area of  $A_1 \approx 0.7$  nm<sup>2</sup> per phospholipid in the fluid state,<sup>28</sup> the average distance between two incorporated integrins is  $d_i = (A_1/X_i)^{0.5}$ .

To avoid non-specific binding of RGD ligands, the integrin-containing membranes were incubated with a 3 wt% solution of bovine serum albumin (BSA) in 20 mM Tris, 150 mM NaCl, 1 mM CaCl<sub>2</sub>, 1 mM MgCl<sub>2</sub>, and 1 mM NaN<sub>3</sub> (pH 7.4) for 1 h. Finally, the sample was rinsed with the same buffer to remove non-adsorbed BSA.

Giant vesicles consist of an equimolar mixture of DMPC and cholesterol, 1 or 2 mol% of 1,2-dimyristoyl-*sn*-glycero-3-phosphoethanolamine-*n*-[methoxy(polyethylene glycol)-2000] (PEG lipid, purchased from Avanti Polar Lipids, Alabaster, USA) and 1 mol% of the cyclic RGD lipopeptide c[Arg-Gly-Asp-D-Phe-Lys-([dimyristoyl-3-thioglycerol-succinimido-propanoyl]Ahx-Gly-Gly)-Gly] (RGD lipid<sup>14</sup>). Giant lipid

vesicles (diameter: 10–20  $\mu\text{m}$ ) were prepared by the electroswelling technique in the presence of a 170 mM sucrose solution under an AC field of 10 Hz and 1 A for 2 h.<sup>20,29</sup> 200  $\mu\text{l}$  of the obtained giant vesicle suspension was injected into the measuring chamber, filled with 10 mM 4-(2-hydroxyethyl) piperazine-1-ethanesulfonic acid (Hepes), 100 mM NaCl, 1 mM  $\text{CaCl}_2$ , 1 mM  $\text{MgCl}_2$ , and 1 mM  $\text{NaN}_3$  (pH 7.4, 205 mOsm). The vesicles settled on the bottom of the measuring chamber due to the higher density of the intravesicular sucrose solution with respect to the outer buffer ( $\Delta\rho = 49.5 \text{ kg m}^{-3}$ ), and due to an osmotic pressure difference of 30 to 40 mOsm between the inside and the outside of the membrane, the vesicles were deflated. Here, the excess surface area generated by deflation enables the vesicles to adhere on planar surfaces.

## Acknowledgements

This work was financially supported by the Deutsche Forschungsgemeinschaft (SFB 563) and the Fonds der Chemischen Industrie. M.T. is thankful to the DFG for the Emmy Noether fellowship (Ta259/1).

## References

- 1 A. A. Brian and H. M. McConnell, *Proc. Natl. Acad. Sci. U. S. A.*, 1984, **81**, 6159.
- 2 A. Grakoui, S. K. Bromley, C. Sumen, M. M. Davis, A. S. Shaw, P. M. Allen and M. L. Dustin, *Science*, 1999, **285**, 221.
- 3 E. Sackmann, *Science*, 1996, **271**, 43.
- 4 M. Tanaka and E. Sackmann, *Nature*, 2005, **437**, 656.
- 5 J. T. Groves and M. L. Dustin, *J. Immunol. Methods*, 2003, **278**, 19.
- 6 E. Sackmann and M. Tanaka, *Trends Biotechnol.*, 2000, **18**, 58.
- 7 M. Tanaka, *MRS Bull.*, 2006, **31**, 513.
- 8 O. Purrucker, A. Förtig, R. Jordan and M. Tanaka, *ChemPhysChem*, 2004, **5**, 327.
- 9 A. Förtig, R. Jordan, K. Graf, G. Schiavon, O. Purrucker and M. Tanaka, *Macromol. Symp.*, 2004, **210**, 329.
- 10 R. Jordan, K. Martin, H. J. Räder and K. K. Unger, *Macromolecules*, 2001, 34.
- 11 O. Purrucker, A. Förtig, R. Jordan, E. Sackmann and M. Tanaka, *Phys. Rev. Lett.*, in print.
- 12 R. Hynes, *Cell*, 1992, **69**, 11.
- 13 S. Gönnerwein, M. Tanaka, B. Hu, L. Moroder and E. Sackmann, *Biophys. J.*, 2003, **84**, 646.
- 14 B. Hu, D. Finsinger, K. Peter, Z. Guttenberg, M. Bärmann, H. Kessler, A. Escherich, L. Moroder, J. Böhm, W. Baumeister, S. Sui and E. Sackmann, *Biochemistry*, 2000, **39**, 12284.
- 15 G. I. Bell, M. Dembo and P. Bongrand, *Biophys. J.*, 1984, **45**, 1051.
- 16 R. Bruinsma, A. Behrisch and E. Sackmann, *Phys. Rev. E*, 2000, **61**, 4253.
- 17 E. Sackmann and R. F. Bruinsma, *ChemPhysChem*, 2002, **3**, 262.
- 18 A. S. G. Curtis, *J. Cell Biol.*, 1964, **20**, 199.
- 19 J. Rädler and E. Sackmann, *J. Phys. II*, 1993, **3**, 727.
- 20 A. Albersdörfer, T. Feder and E. Sackmann, *Biophys. J.*, 1997, **73**, 245.
- 21 R. Bruinsma, Adhesion and Rolling of Leukocytes. A Physical Model, in *Proceedings of the NATO Advanced Institute of Physics and Biomaterials, NATO Advanced Study Institute Series B: Physics*, Kluwer, London, 1995.
- 22 R. B. Gennis, *Biomembranes – Molecular Structure and Function*, Springer, New York, 1989.
- 23 Z. Guttenberg, A. R. Bausch, B. Hu, R. Bruinsma, L. Moroder and E. Sackmann, *Langmuir*, 2000, **16**, 8984.
- 24 O. Purrucker, A. Förtig, K. Lüdtko, R. Jordan and M. Tanaka, *J. Am. Chem. Soc.*, 2005, **127**, 1258.
- 25 M. Bradford, *Anal. Biochem.*, 1976, **72**, 248.
- 26 C. H. Fiske and Y. Subbarow, *J. Biol. Chem.*, 1925, **66**, 375.
- 27 G. Bartlett, *J. Biol. Chem.*, 1958, **234**, 466.
- 28 D. Marsh, *Handbook of Lipid Bilayers*, CRC Press, Boca Raton, FL, 1990.
- 29 D. Dimitrov and M. Angelova, *Bioelectrochem. Bioenerg.*, 1988, **19**, 323.